Geotech Geol Eng (2017) 35:445–461
DOI 10.1007/s10706-016-0119-2

ORIGINAL PAPER

Prediction of Laboratory Peak Shear Stress Along the Cohesive Soil–Geosynthetic Interface Using Artificial Neural Network

Prasenjit Debnath · Ashim Kanti Dey

Received: 6 March 2016 / Accepted: 31 October 2016 / Published online: 7 November 2016

Abstract In general, soil–geosynthetic interface behaviour is modeled by interface element which involves the assumption of stiffness values which are difficult to determine experimentally. Most of the geosynthetic-reinforced earth structures fail at the interface of the geosynthetic and the soil due to slip or plastic yielding of the reinforced soil. Hence, for a proper design of the soil–geosynthetic interface, an artificial neural network (ANN) model can be used as an alternative approach for the prediction of the soil–geosynthetic interface behavior. The present study uses an ANN model to predict the peak shear stress along the cohesive soil–geosynthetic interface. Three-layer feed-forward back-propagation neural networks with 4, 10 and 15 hidden nodes using three different learning algorithms are examined. Out of three learning algorithms, Bayesian regularization learning algorithm with four hidden nodes is used for its highest coefficient of determination ($R^2 = 0.988$) for the testing set and all of the predicted data falling within the 99% prediction interval. The prediction performance of the ANN model with Bayesian regularization learning algorithm with four hidden nodes is compared with the multi-variable regression analysis. Different sensitivity analyses to quantify the most importance input parameters are also discussed. A neural interpretation diagram to visualize the effect of input parameters on the output is presented. Finally, a predicted model equation is obtained based on the neural network parameters.

Keywords Artificial neural network · Peak shear stress · Sensitivity analysis · Multi-variable regression · Statistical analysis

P. Debnath (✉) · A. K. Dey
Department of Civil Engineering, NIT Silchar, Silchar 788010, India
e-mail: prasen458@gmail.com

A. K. Dey
e-mail: akdey@civil.nits.ac.in

1 Introduction

In general practice, modeling of soil–geosynthetic interface behavior is done by introducing interface elements. This can be accomplished by a number of ways like, node compatibility spring element; composite layer model; joint element of zero or non-zero thickness; etc. (Andrawes et al. 1982; Love et al. 1987; Gens et al. 1988; Poran et al. 1989; Burd and Brocklehurst 1990; Wilson-Fahmy and Koerner 1993; Abdel-Baki and Raymond 1994; Yamamoto and Otani 2002). But all these methods involve horizontal and vertical stiffness values which are very difficult to determine experimentally. To overcome this difficulty Poulos and Davis (1974) and Basudhar et al. (2008) modeled interface as a contact problem and assumed that failure would occur due to a slip at the interface between the soil and the geosynthetic and

not due to yielding of the reinforced soil. It is very essential to provide an accurate estimate of the properties of the interface for an accurate prediction. The properties of the soil–geosynthetic interface depend on many factors, like, nature of force along the interface (direct shear or pullout mode); physical and mechanical properties of the soil (density, grain shape and size, grain size distribution, moisture content, cohesive strength, frictional angle, etc.), mechanical properties of the geosynthetic (ultimate tensile strength, stress at 5% strain) and shape and geometry of the geosynthetic. However, the most important parameters are the density of the soil, moisture content of the soil, soil–geosynthetic adhesion, soil–geosynthetic interface frictional angle, properties of the geosynthetic and normal stress on the shear plane. It is observed that the interface shear resistance at the high density polyethylene (HDPE)–clay interface is maximum when the clay is in the compacted condition and minimum when the clay is near saturation (Mitchell et al. 1990; Lopes 2002). Previous studies conducted at the Louisiana Transportation Research Center (LTRC) on geogrid reinforcement in cohesive soils also showed that increased moisture content resulted in decreased pullout resistance (Farrag and Morvant 2003a, b). Large direct shear tests showed that increase in molding moisture content and/or decrease in dry density caused an appreciable reduction in the cohesive soil–geosynthetic interface shear resistance (Farrag and Griffin 1993; Farrag 1995; Farsakh et al. 2007).

Even though these methods are widely used, reliable predictions are uncertain due to the variability of soil properties. To overcome the problem, ANN model can be used as a suitable alternative. Since it is a data driven process, it can learn from history. It can also adapt to any anomaly which gets unnoticed by most of the traditional techniques for the prediction of soil–geosynthetic interface behavior. Several researchers have used the ANN model to predict different soil behaviours like skin friction of the piles in clay (Goh 1995); ultimate bearing capacity of piles (Lee and Lee 1996); slope stability prediction (Sakellariou and Ferentinou 2005); undrained lateral load capacity of piles (Das and Basudhar 2006); the residual frictional angle of clay (Das and Basudhar 2008); elastic modulus of jointed rock mass (Maji and Sitharam 2008); prediction models for soil compaction and permeability (Sinha and Wang 2008); modeling sulfuric acid induced swell in carbonate clays (Sivapullaiah et al. 2009); the compression index of soils (Park and Lee 2011); effective stress parameters of unsaturated soils (Ajdari et al. 2012); ground settlement prediction (Kanayama et al. 2014); prediction of unconfined compressive strength of geopolymer stabilized clayey soil (Mozumder and Laskar 2015) etc.

From the above study it can be observed that the ANN has been used successfully in solving various geotechnical engineering problems. The detailed discussion of ANN is refrained in the present study and can be found in the literature (Minsky and Papert 1969; Lippman 1987; DARPA 1988; Caudill 1989; Caudill and Butler 1992). The ANN is considered as a black box system as it is unable to explain the fundamental principles of prediction. Therefore, interpretation of weights may be considered the subject of future research (Goh et al. 2005). Keeping in mind the above limitations the present study uses a feed forward back propagation neural network model with 4, 10 and 15 hidden nodes to predict the peak shear stress at the cohesive soil–geosynthetic interface. Three learning algorithms, namely Bayesian regularization (BR), Levenberg–Marquardt (LM) and scaled conjugate gradient (SCG) have been used. A comparison study has been done to obtain the best learning algorithm. Sensitivity analysis is employed to quantify the important input parameters for prediction of the peak shear stress (PSS).

2 Development of Prediction Model

2.1 Development of ANN Model

The ANN process mainly consists of four steps, namely, collection of data, selection of a network type, selection of a learning algorithm and selection of a criterion for stopping the process. In the present study, the data are taken from the research paper of Farsakh et al. (2007). The data consist of dry density of cohesive soil (γ), moisture content of cohesive soil in percentage (%w), normal stress on the shear plane (σ_n), soil–geosynthetic adhesion (c_a) and soil–geosynthetic interface frictional angle (δ) as the inputs and peak shear stress at cohesive soil–geosynthetic interface (T) as the output. Similar approach of input–output pattern has already been studied by other

researchers (Monjezi et al. 2006; Sarkar et al. 2010; Sobhani et al. 2010; Yaprak et al. 2013). In the present study, out of 90 data points, 70% are considered for training the ANN model (shown in Table 1) and rest 30% for testing the model (shown in Table 2) as suggested by Shahin et al. (2004). Statistical parameters of the training and testing data are given in Table 3. Since the input parameters have different units of measure, normalization of their values is necessary, hence all the variables (inputs and output) are normalized in the range [−1, 1]. ANN model has been implemented in MATLAB R2013a environment with neural network toolbox, with three different learning algorithms as mentioned above. A three-layer feed-forward back-propagation neural network with one hidden layer is adopted as suggested by previous researchers (Rumelhart et al. 1986; Lippman 1987; Sonmez et al. 2006) while the number of hidden neurons is determined using a heuristic model as suggested by Sonmez et al. (2006). The heuristic model is shown in Table 4. The model shows that the hidden neurons may vary from 1 to 15. Figure 1 shows the relationship between the numbers of neurons against MSE during the training. It is observed from the figure that 4, 10 and 15 numbers of hidden neurons give the optimum architecture of ANN model based on the minimum value of mean square error (MSE) of the training data set. Hence, in the present study the optimum numbers of hidden neurons are taken as 4, 10 and 15. Once network weights and biases are initialized randomly, training of the network starts. Hyperbolic sigma transfer function is used as the transfer function for calculating the output from a certain neuron from its inputs. During training, the progress is constantly updated in the training window. The major challenge in the successful application of ANN is when to stop the training. If training is inadequate, then the network will not be fully trained, whereas if training is extreme then it will memorize the training pattern or learn noise. Normally the network stops when gradient of performance reaches a threshold value or when the number of failed validation reaches a prefixed number or when the number of epoch reaches a certain specified number. The gradient will become very small as the training reaches a minimum of the performance and validation checks represent the number of successive iterations that the validation performance fails to decrease. An epoch is a cycle of forward and backward process through which the network weights and biases are modified. For the present study, the stopping criterion for the number of epoch is 1000, the magnitude of gradient of performance is 10^{-7} and the number of failed validation checks is 6.

The performance of ANN model is reported in terms of five statistical parameters, namely the coefficient of determination (R^2), mean square error (MSE), mean absolute percentage error (MAPE), variance absolute relative error (VARE) and median absolute error (MEDAE).

2.1.1 *Bayesian Regularization (BR) Learning Algorithm*

To advance the generalization capabilities of the conventional back-propagation algorithm MacKay (1991) and Neal (1992) introduce Bayesian back propagation neural networks. It is based on the Bayesian statistical approach (Box and Tiao 1973) and originated in the field of highest entropy (Gull 1988). To create a well generalized network, the Bayesian regularization learning algorithm involves constraining the number of the network parameters through a regularized that penalizes the more complex weight functions in favor of simpler functions. This procedure is carried out by adding a penalty term to the sum squared error. Instead of just giving a single "optimum" prediction, the Bayesian approach provides a probability distribution over the predicted value. This is frequently very important as it provides information on the characteristic error of the prediction that arises from the uncertainty associated with interpolating noisy data. In order to create a prediction model with the most accurate response, three artificial neural networks with 4, 10 and 15 hidden neurons are developed. Comparison of predicted peak shear stress, PSS (Y), with experimental peak shear stress, PSS (T), for training and testing sets, using ANN with 4, 10 and 15 hidden neurons, is shown in Fig. 2. From the figures it is observed that the ANN model with four hidden neurons gives the highest correlation coefficient R being equal 0.995 for the training set and 0.994 for the testing set. The standard error is also observed to be the smallest, 1.11 and 1.14 respectively as shown in Fig. 2a, b. In order to validate the predicted PSS values obtained from proposed ANN model with experimental values, a 99% prediction interval is chosen. 99% prediction interval is defined as an

Table 1 Summary of training data for peak shear stress of soil geosynthetics interface (from Farsakh et al. 2007)

Sl. no.	Soils and geosynthetics	γ (kN/m^3)	w (%)	σ_n (kPa)	c_a (kPa)	δ (°)	T (kPa)
Training data							
1	Clay 6 and BX-6100	15.08	12	50	12.7	27.7	38.9
2	Clay 6 and BX-6100	15.25	18.8	25	1	15.4	7.9
3	Clay 6 and BX-6100	15.25	18.8	50	1	15.4	14.8
4	Clay 6 and BX-6100	15.25	18.8	75	1	15.4	21.7
5	Clay 6 and BX-6100	16.70	18.8	25	12.6	11.5	17.7
6	Clay 6 and BX-6100	16.70	18.8	50	12.6	11.5	22.8
7	Clay 6 and BX-6100	16.70	18.8	75	12.6	11.5	34.8
8	Clay 6 and BX-6100	17.63	18.8	75	11.7	21.2	40.8
9	Clay 6 and BX-6100	16.27	21	25	4.7	12.2	10.1
10	Clay 6 and BX-6100	16.27	21	75	4.7	12.2	21
11	Clay 6 and geotextiles	15.08	12	25	13.5	22.8	24
12	Clay 6 and geotextiles	15.08	12	75	13.5	22.8	48.9
13	Clay 6 and geotextiles	15.25	18.8	50	4.7	19.6	22.5
14	Clay 6 and geotextiles	15.25	18.8	75	4.7	19.6	34.1
15	Clay 6 and geotextiles	16.70	18.8	25	3.7	25.5	15.6
16	Clay 6 and geotextiles	16.70	18.8	50	3.7	25.5	27.5
17	Clay 6 and geotextiles	17.63	18.8	25	19.2	18.6	27.6
18	Clay 6 and geotextiles	17.63	18.8	50	19.2	18.6	36
19	Clay 6 and geotextiles	16.27	21	25	4.4	21.8	14.4
20	Clay 6 and geotextiles	16.27	21	50	4.4	21.8	24.4
21	Clay 6 and geotextiles	16.27	21	75	4.4	21.8	32.7
22	Clay 25 and BX-6100	16.01	11	75	12	31.5	57.9
23	Clay 25 and BX-6100	15.00	16.5	50	2.9	14.4	15.7
24	Clay 25 and BX-6100	15.00	16.5	75	2.9	14.4	22.1
25	Clay 25 and BX-6100	17.25	16.5	25	8.9	21.4	18.7
26	Clay 25 and BX-6100	17.25	16.5	50	8.9	21.4	28.5
27	Clay 25 and BX-6100	18.98	16.5	25	5.5	28.2	18.9
28	Clay 25 and BX-6100	18.98	16.5	50	5.5	28.2	32.3
29	Clay 25 and BX-6100	18.98	16.5	75	5.5	28.2	45.6
30	Clay 25 and BX-6100	16.86	20	50	7.1	10.6	16.5
31	Clay 25 and BX-6100	16.86	20	75	7.1	10.6	21.3
32	Clay 25 and geotextiles	16.01	11	25	16.5	19	25.1
33	Clay 25 and geotextiles	16.01	11	50	16.5	19	33.7
34	Clay 25 and geotextiles	15.00	16.5	25	11	8.9	14.9
35	Clay 25 and geotextiles	15.00	16.5	50	11	8.9	18.8
36	Clay 25 and geotextiles	17.25	16.5	75	12.2	17.5	42
37	Clay 25 and geotextiles	18.98	16.5	25	14	25.6	26
38	Clay 25 and geotextiles	18.98	16.5	50	14	25.6	38
39	Clay 25 and geotextiles	18.98	16.5	75	14	25.6	50
40	Clay 25 and geotextiles	16.86	20	25	9	17.3	16.8
41	Clay 25 and geotextiles	16.86	20	75	9	17.3	36.2
42	Clay 49 and BX-6100	13.05	24	25	12.9	24.5	24.3
43	Clay 49 and BX-6100	13.05	24	75	12.9	24.5	47.1

Table 1 continued

Sl. no.	Soils and geosynthetics	γ (kN/m^3)	w (%)	σ_n (kPa)	c_a (kPa)	δ (°)	T (kPa)
44	Clay 49 and BX-6100	11.36	29.3	25	4.9	19.4	13.7
45	Clay 49 and BX-6100	11.36	29.3	75	4.9	19.4	31.3
46	Clay 49 and BX-6100	13.57	29.3	25	13.9	13.5	19.9
47	Clay 49 and BX-6100	13.57	29.3	50	13.9	13.5	25.9
48	Clay 49 and BX-6100	13.57	33	75	13.9	13.5	31.8
49	Clay 49 and BX-6100	14.58	33	25	16	17.7	24
50	Clay 49 and BX-6100	14.58	29.3	75	16	17.7	40.1
51	Clay 49 and BX-6100	13.14	33	25	5	14.1	11.3
52	Clay 49 and BX-6100	13.14	33	50	5	14.1	17.6
53	Clay 49 and geotextiles	13.05	24	25	21	19.8	30
54	Clay 49 and geotextiles	13.05	24	50	21	19.8	39
55	Clay 49 and geotextiles	13.05	24	75	21	19.8	56
56	Clay 49 and geotextiles	11.36	29.3	50	9.1	16.5	23.9
57	Clay 49 and geotextiles	13.57	29.3	25	8	21.8	18
58	Clay 49 and geotextiles	17.25	16.5	50	8	21.8	28
59	Clay 49 and geotextiles	14.58	29.3	25	19	13.5	25
60	Clay 49 and geotextiles	14.58	29.3	50	19	13.5	31
61	Clay 49 and geotextiles	14.58	29.3	75	19	13.5	42
62	Clay 49 and geotextiles	13.14	33	50	9.5	16.7	24.5
63	Clay 49 and geotextiles	13.14	33	75	9.5	16.7	35

interval within which 99% of Y values for a certain X value will lie around the linear regression line. An established equation (Verschuuren 2007) to obtain the upper and lower bound prediction interval values is used in the present study. Figure 2b shows that all the testing data lie well within the 99% prediction interval band, which confirms the validity of the proposed ANN model. It is clear that ANN model with BR learning algorithm with four hidden nodes gives the most accurate predictions that fall within the 99% prediction interval.

2.1.2 *Levenberg–Marquardt (LM) Learning Algorithm*

The LM learning algorithm is usually considered as the fastest method for training moderate-sized feed-forward neural networks (Singh et al. 2005; Khandelwal and Singh 2010) and it is the best choice for solving the problems of supervised learning, which is the case in the present analysis. Comparison of predicted peak shear stress, PSS (Y), with experimental peak shear stress, PSS (T), for training and testing sets, using ANN with 4, 10 and 15 hidden neurons, is given in Fig. 3. From Fig. 3a–f it is clear that the ANN model with four hidden neurons has the highest correlation coefficient R, and it is obtained as 0.99 for the training set and 0.982 for testing set with a small value of the standard error, SE = 2.33 for testing. It means that the average distance of the data points from the fitted line is 2.33 kPa. Figure 3b also shows that the upper bound and the lower bound correspond to 99% prediction interval i.e. all the data points lie well within the 99% prediction interval band, which confirms the precision of the proposed model.

2.1.3 *Scaled Conjugate Gradient (SCG) Learning Algorithm*

SCG learning algorithm belongs to the group of conjugate gradient optimization methods which are well suited to handle the large-scale problems in a successful way (Fletcher 2000). This method represents one of the four most often used algorithms of this group, besides Polak–Ribiére Update, Fletcher–Reeves Update and Powell–Beale Restarts algorithm.

Table 2 Summary of testing data for peak shear stress of soil geosynthetics interface (from Farsakh et al. 2007)

Sl. no.	Soils and geosynthetics	γ (kN/m^3)	w (%)	σ_n (kPa)	c_a (kPa)	δ (°)	T (kPa)
Testing data							
1	Clay 6 and BX-6100	15.08	12.00	25.00	12.70	27.70	25.80
2	Clay 6 and BX-6100	15.08	12.00	75.00	12.70	27.70	52.10
3	Clay 6 and BX-6100	17.63	18.80	25.00	11.70	21.20	21.40
4	Clay 6 and BX-6100	17.63	18.80	50.00	11.70	21.20	31.10
5	Clay 6 and BX-6100	16.27	21.00	50.00	4.70	12.20	15.50
6	Clay 6 and geotextiles	15.08	12.00	50.00	13.50	22.80	34.50
7	Clay 6 and geotextiles	15.25	18.80	25.00	4.70	19.60	13.60
8	Clay 6 and geotextiles	16.70	18.80	75.00	3.70	25.50	37.50
9	Clay 6 and geotextiles	17.63	18.80	75.00	19.20	18.60	48.80
10	Clay 25 and BX-6100	16.01	11.00	25.00	12.00	31.50	27.30
11	Clay 25 and BX-6100	16.01	11.00	50.00	12.00	31.50	42.60
12	Clay 25 and BX-6100	15.00	16.50	25.00	2.90	14.40	9.30
13	Clay 25 and BX-6100	17.25	16.50	75.00	8.90	21.40	38.30
14	Clay 25 and BX-6100	16.86	20.00	25.00	7.10	10.60	11.80
15	Clay 25 and geotextiles	16.01	11.00	75.00	16.50	19.00	44.30
16	Clay 25 and geotextiles	15.00	16.5	75	11	8.9	29.2
17	Clay 25 and geotextiles	17.25	16.5	25	12.2	17.5	20.1
18	Clay 25 and geotextiles	17.25	16.5	50	12.2	17.5	28
19	Clay 25 and geotextiles	16.86	20	50	9	17.3	24.6
20	Clay 49 and BX-6098	13.05	24	50	12.9	24.5	35.7
21	Clay 49 and BX-6101	11.36	29.3	50	4.9	19.4	22.5
22	Clay 49 and BX-6107	14.58	29.3	50	16	17.7	32
23	Clay 49 and BX-6111	13.14	33	75	5	14.1	23.8
24	Clay 49 and geotextiles	11.36	29.3	25	9.1	16.5	16.5
25	Clay 49 and geotextiles	11.36	29.3	75	9.1	16.5	33.6
26	Clay 49 and geotextiles	13.57	33	75	8	21.8	39
27	Clay 49 and geotextiles	13.14	33	25	9.5	16.7	17

Table 3 Statistical parameters of training and testing data of ANN model

Model variable	γ	%w	σ_n	c_a	δ	T
Standard deviation						
Training data	1.97	6.33	20.58	5.57	5.36	11.33
Testing data	1.96	7.62	20.80	4.10	5.72	11.36
Mean						
Training data	15.50	21.28	50.00	10.27	18.59	27.88
Testing data	15.10	20.86	50.00	10.11	19.75	28.74
Maximum						
Training data	18.98	33.00	75.00	21.00	31.50	57.90
Testing data	17.63	33.00	75.00	19.20	31.50	52.10
Minimum						
Training data	11.36	11.00	25.00	1.00	8.90	7.90
Testing data	11.36	11.00	25.00	2.90	8.90	9.30
Range						
Training data	7.62	22	50	20	22.6	50
Testing data	6.27	22	50	16.3	22.6	42.8

Table 4 Different heuristics used for calculate the number of nodes in hidden layer (from Sonmez et al. 2006)

Heuristic	Calculated number of nodes for this study
$\leq 2 \times N_i + 1$	≤ 11
$3 \times N_i$	15
$\frac{2 + N_o \times N_i + 0.5N_o \times \left(N_o^2 + N_i\right) - 3}{N_i + N_o}$	1
$2N_i/3$	4
$2N_i$	10
$(N_i + N_o)/2$	3
$\sqrt{(N_i + N_o)}$	3

N_i represents number of input nodes, N_o represent number of output nodes

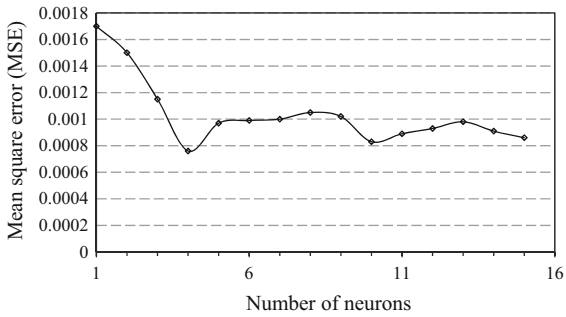

Fig. 1 Relationship between the number of neurons and MSE

Each one of these conjugate gradient algorithms requires a line search at every iteration step, which is computationally expensive, since the network reply to all training inputs has to be computed several times for each search. The SCG algorithm was designed to avoid this time-consuming process, by combining the model-trust region approach (used in LM algorithm) with the conjugate gradient algorithm (Moller 1993). Comparison of predicted peak shear stress, PSS (Y), with experimental peak shear stress, PSS (T), for training and testing sets, using ANN with 4, 10 and 15 hidden neurons, is given in Fig. 4. From Fig. 4a–f it is clear that the ANN model with four hidden neurons has the highest correlation coefficient R, obtained as 0.994 for the training set and 0.988 for testing set with a small value of the standard error, SE = 1.96 for testing. It means that the average distance of the data points from the fitted line is 1.96 kPa. Figure 4b shows that the upper bound and the lower bound correspond to 99% prediction interval i.e. all the data points lie well within the 99% prediction interval band, which confirms the precision of the proposed model.

2.2 MVR Model Development

In the present study, a multi-variable regression analysis (MVR) is also conducted to predict the peak shear stress of the soil geosynthetic interface. Similar to ANN model, 70% of the total data are used for developing the MVR model. Rest 30% data are used to evaluate the prediction efficacy of the model. The generalized linear relationship between the dependent variable and the independent variables takes the form as shown in Eq. (1).

$$Y = c_0 + c_1X_1 + c_2X_2 + c_3X_3 + \cdots + c_nX_n \pm e \quad (1)$$

where Y is dependent variable, c_0 is the Y intercept. c_1, c_2, c_3 and c_n are the slopes associated with the independent variables X_1, X_2, X_3 and X_n and e is the error. MVR model is developed with T as dependent variable and γ, $\%w$, σ_n, c_a and δ as independent variables.

3 Performance Evaluation of the Proposed ANN Model

Performances of the developed prediction models can be further evaluated using different standard statistical criteria given in Table 5 (Monjezi et al. 2013). Calculated statistical errors are shown in Table 6. The ANN model with BR learning algorithm with four hidden nodes has the highest value of coefficient of determination R^2 and lowest values of mean square error (MSE), mean absolute percentage error (MAPE), median absolute error (MEDAE) and variance absolute relative error (VARE), in comparison with other proposed ANN models. The optimum architecture of ANN model was characterized by four neurons in hidden layer with hyperbolic tangent sigmoid function

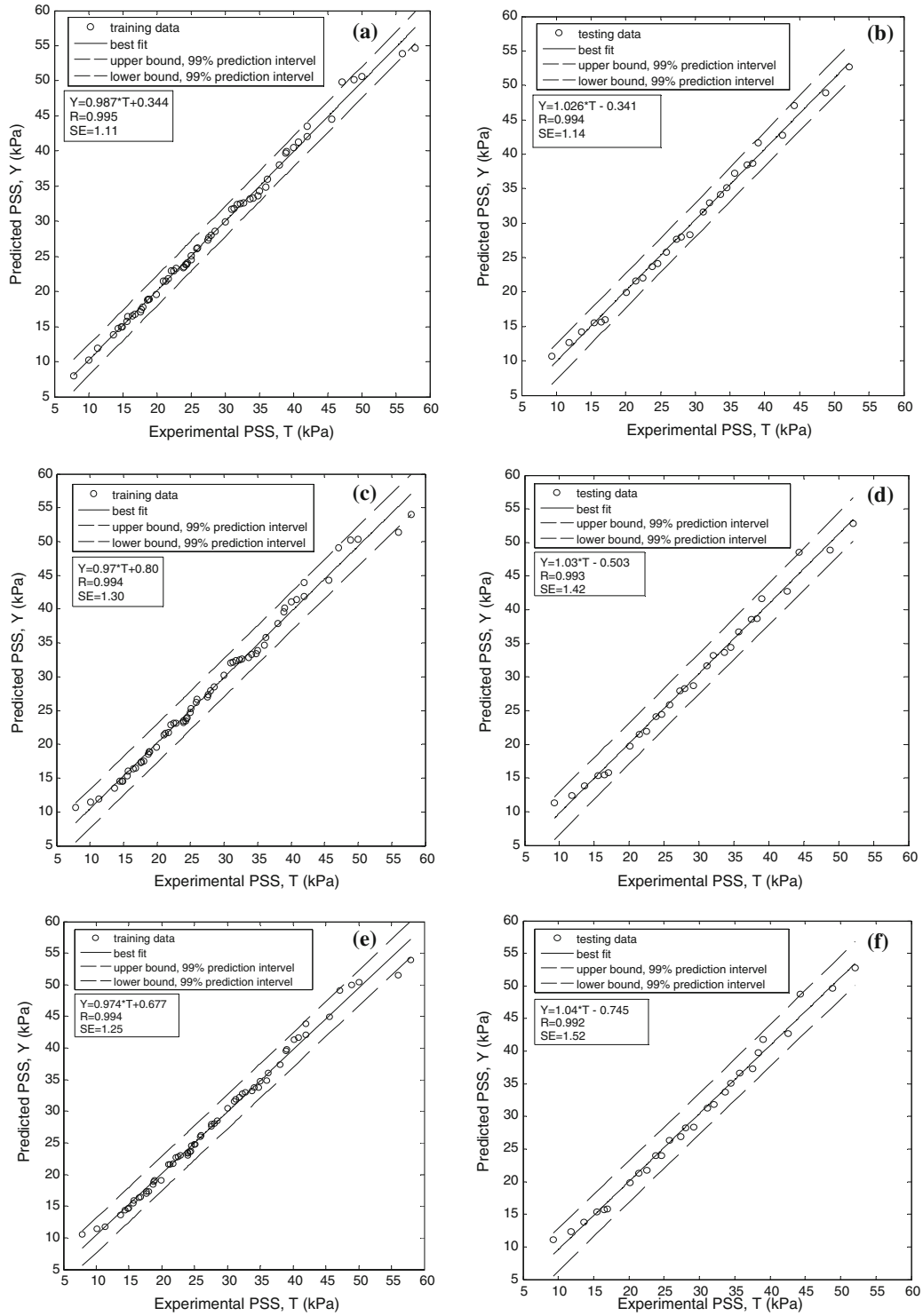

Fig. 2 Comparison of predicted and experimental values of peak shear stress (kPa) for training and testing sets using Bayesian regularization learning algorithm. **a** Comparison with 4 hidden nodes for training data, **b** comparison with 4 hidden nodes for testing data, **c** comparison with 10 hidden nodes for training data, **d** comparison with 10 hidden nodes for testing data, **e** comparison with 15 hidden nodes for training data, **f** comparison with 15 hidden nodes for testing data

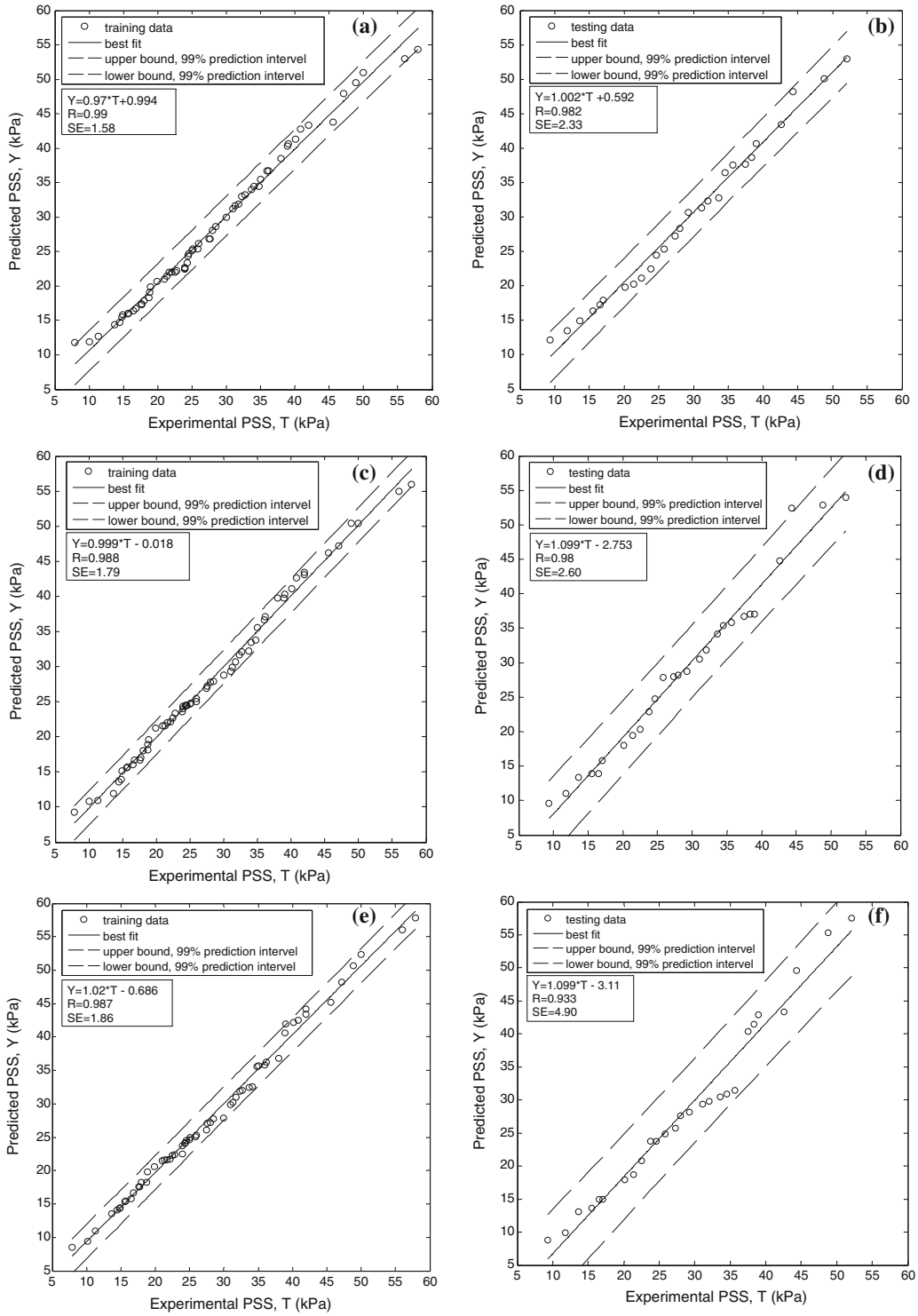

Fig. 3 Comparison of predicted and experimental values of peak shear stress (kPa) for training and testing using Levenberg–Marquardt learning algorithm. **a** comparison with 4 hidden nodes for training data, **b** comparison with 4 hidden nodes for testing data, **c** comparison with 10 hidden nodes for training data, **d** comparison with 10 hidden nodes for testing data, **e** comparison with 15 hidden nodes for training data, **f** comparison with 15 hidden nodes for testing data

as the transfer function and a pure linear transfer function at the output layer. Out of three learning algorithms Bayesian regularization back propagation learning algorithm is used for its better generalization for the training data and lowest statistical error.

4 Results and Discussions of ANN and MVR Models

From Table 6 it is observed that out of three types of ANN model, The Bayesian regularization (BR) model with four hidden neurons is the best one showing higher value of R^2 and lesser values of statistical errors. These results are compared with MVR model in Table 7. R^2, MSE, MAPE, VARE and MEDAE value of the BR model for training and testing data are found to be 0.991, 1.21, 2.43, 1.17 and 0.53 & 0.988, 1.48, 3.31, 1.27 and 0.60 respectively, while for MVR model these values are found to be 0.956, 5.52, 8.04, 6.54 and 1.45 & 0.965, 4.73, 7.08, 5.58 and 0.93 respectively. The statistical values in Table 7 suggest that the ANN model is superior to MVR model in learning and predicting the experimental data. The analysis of variance (ANOVA) and statistical information of predictor variables of MVR model are shown in Tables 8 and 9. Regression analysis data in Tables 8 and 9 are made with the help of *t* test and F-test at 95% confidence level. From Table 8, it is observed that the *P* value (2.01E−37) is very small which suggests that the confidence level i.e. $(1 - P)$ is almost 100% and at least one of the coefficients of MVR model is important. However, to identify the significant coefficients in the MVR model in addition to F-test, *t* tests are conducted. The t-stat and corresponding *P* values of individual coefficients are given in Table 9. It is observed that *P* values of coefficients of γ and %w are very high with corresponding low confidence levels $[(1 - P) < 0.95]$ and hence these coefficients are insignificant for the MVR model. On the other hand *P* values of σ_n, c_a and δ are very low with high confidence level $[(1 - P) > 0.95]$ and hence it is proposed that these coefficients are significant in MVR model. Lower and upper limits of 95% confidence interval are also shown in Table 9. Confidence intervals of γ and %w include zero falls and hence are not consistent with the significance of *t* test. Confidence intervals of σ_n, c_a and δ do not include zero and hence are consistent with the significance of *t* tests. It is evident that MVR model fails to generalize the cohesive soil–geosynthetic interface mechanism as it rejects the significance of γ, and %w in PSS prediction.

5 Sensitivity Analysis

Sensitivity analysis is a major concern for selecting the important input variables. Different methods have been subjected to select the significant input variables. However, methods such as Garson's algorithm and Connection weight approach have been successfully used by some researchers for assessing the variable contribution in geotechnical engineering problems (Goh 1994; Das and Basudhar 2006, 2008; Das et al. 2011). In the present study, aforementioned two methods have been used to identify significant input variables in PSS prediction. Both the approaches use optimized weight vector to identify the important input variables, details of which are available in the literature (Garson 1991; Olden and Jackson 2002). Optimized weight vectors of the ANN model are presented in Table 10. Based on the weights listed in Table 10 the importance and relative ranking of different input variables of ANN using Garson's algorithm and Connection weight approach are shown in Table 11. It is observed from Table 11 that both the approaches namely Garson's algorithm and Connection weight approach rank normal stress (σ_n) as the most important parameter. However, the Connection weight approach ranks percentage water content (%w) as the least important parameter whereas; Garson's algorithm ranks dry density (γ) as the least important parameter. However it is to be mentioned here that researchers have shown an indirect effect of soil moisture content and direct effect of dry density on cohesive soil–geosynthetics interaction (Farsakh et al. 2007). The interface efficiency decreases with the increase in moisture content and decreasing dry density. The results of the present study showed that out of five input parameters chosen, the dry density and moisture content have the least effect on peak shear stress at cohesive soil–geosynthetics interface.

Ranking given by connection weight approach seems to be more realistic and acceptable due to following reasons:

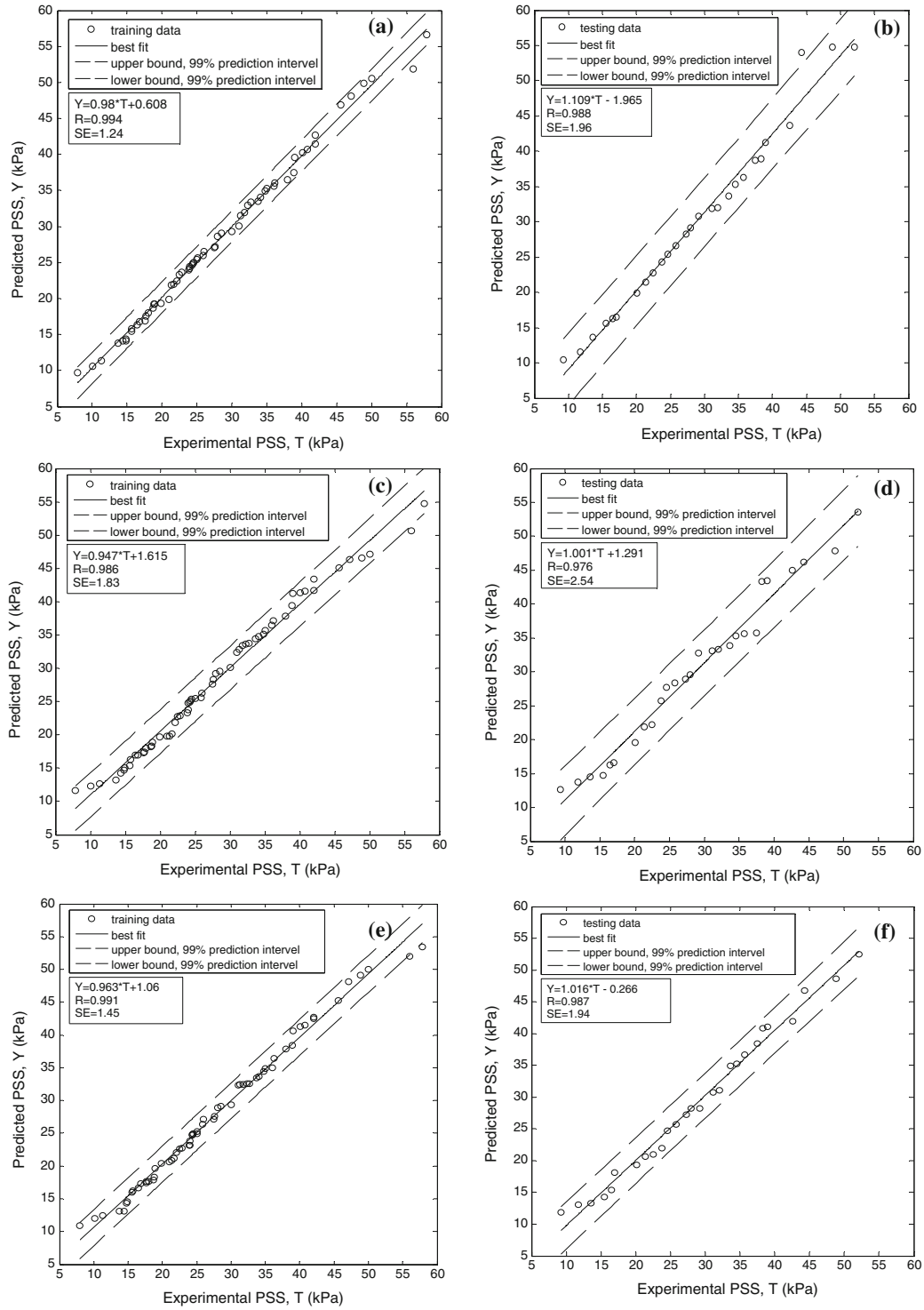

Fig. 4 Comparison of predicted and experimental values of peak shear stress (kPa) for training and testing sets using *Scaled conjugate gradient learning algorithm*. **a** Comparison with 4 hidden nodes for training data, **b** comparison with 4 hidden nodes for testing data, **c** comparison with 10 hidden nodes for training data, **d** comparison with 10 hidden nodes for testing data, **e** comparison with 15 hidden nodes for training data, **f** comparison with 15 hidden nodes for testing data

Table 5 Statistical error formulation used for models' evaluation (from Monjezi et al. 2013)

Statistical parameter	Equation
Mean square error (MSE)	$MSE = \frac{1}{n} \times \left[\sum_{i=1}^{n} \lvert t_i - x_i \rvert^2\right]$
Mean absolute percentage error (MAPE)	$MAPE = \frac{1}{n} \times \left[\sum_{i=1}^{n} \left\lvert \frac{t_i - x_i}{t_i} \right\rvert\right] \times 100$
Variance absolute relative error (VARE)	$VARE = \frac{1}{n} \times \left[\sum_{i=1}^{n} \left(\left\lvert \frac{t_i - x_i}{t_i} \right\rvert - mean \left\lvert \frac{t_i - x_i}{t_i} \right\rvert^2 \right)\right]$
Median absolute error (MEDAE)	$MEDAE = median(t_i - x_i)$

Table 6 Statistical errors of different models for predicting PSS

ANN model			Statistical errors			
Learning algorithms	No. of hidden nodes	R^2	MSE	MAPE	VARE	MEDAE
Bayesian regularization	4	0.988	1.48	3.31	1.27	0.60
	10	0.986	2.21	3.81	1.81	0.602
	15	0.984	2.45	3.82	2.35	0.606
Levenberg–Marquardt	4	0.964	5.46	7.31	5.52	1.42
	10	0.96	7.48	8.00	6.21	1.73
	15	0.871	23.52	11.72	10.72	2.34
Scaled conjugate gradient	4	0.977	6.47	3.88	2.09	0.64
	10	0.954	7.73	8.21	6.42	1.49
	15	0.973	3.58	6.18	5.18	1.31

Table 7 Performance of ANN and MVR model

Model	Dataset	R^2	Statistical parameter			
			MSE	MAPE	VARE	MEDAE
ANN	Training data	0.991	1.21	2.43	1.17	0.53
	Testing data	0.988	1.48	3.31	1.27	0.60
MVR	Training data	0.956	5.52	8.04	6.54	1.45
	Testing data	0.965	4.73	7.08	5.58	0.93

Table 8 Analysis of variance (ANOVA) of MVR model

Source	*df*[a]	SS[b]	MS[c]	F	*P*
Regression	5.000	7616.879	1523.376	249.654	2.01E−37
Residual	57.000	347.811	6.102		
Total	62.000	7964.691			

[a] Degree of freedom

[b] Sum square

[c] Mean square

- With the increase in normal stress the confining pressure at the cohesive soil–geosynthetic interface is increased which causes an increase in the interface efficiency resulting in higher value of PSS. Farsakh et al. (2007) also showed that with increase in normal stress and keeping the dry

Table 9 Statistical information of predictor variable of MVR model

Predictor variable	Coefficients	Standard error	*t* stat	*P* value	Lower 95%	Upper 95%
Intercept	−15.699	4.643	−3.381	0.001	−24.997	−6.401
γ	−0.187	0.214	−0.873	0.386	−0.617	0.242
%w	−0.088	0.068	−1.285	0.204	−0.224	0.049
σ_n	0.381	0.015	24.929	0.000	0.350	0.411
c_a	1.119	0.057	19.746	0.000	1.005	1.232
δ	0.959	0.063	15.217	0.000	0.833	1.085

Table 10 Connection weights and biases for predicting PSS with Bayesian learning algorithm with four hidden nodes

Neuron	Weights						Biases	
	Input 1	Input 2	Input 3	Input 4	Input 5	Output	Hidden layer	Output layer
Hidden neuron 1	0.2241	−0.1281	0.5307	−0.1079	0.4599	0.7687	−0.611	−0.1726
Hidden neuron 2	0.0354	0.2943	1.0981	−0.4282	−0.0225	0.5707	0.0486	
Hidden neuron 3	0.0175	0.3211	0.3505	−0.5339	−0.3239	−0.9582	−0.3116	
Hidden neuron 4	−0.1136	−0.2624	−0.0649	−0.5137	−0.0691	−0.7049	−0.2448	

Table 11 Sensitivity analysis results

Input	Garson's algorithm (%)		Connection weight approach	
Parameters	Relative importance	Ranking of inputs as per relative importance	Relative importance	Ranking of inputs as per relative importance
γ	7.3900	5	0.26	4
w	17.7200	3	−0.05	5
σ_n	31.0100	1	0.74	1
c_a	28.7300	2	0.55	3
δ	15.1500	4	0.70	2

density and moisture content constant, the PSS increases. Therefore, ranking of the normal stress as the most important parameter for PSS as per connecting weight approach is confirmed.

- Using Mohr–Coulomb failure criteria following equation is deduced (Farsakh et al. 2007):

$$\tau_{s-g} = c_a + \sigma_n \tan\delta \quad (2)$$

where τ_{s-g} is the shear stress along the soil–geosynthetic interface.

Equation (2) clearly shows that shear stress is directly related to soil–geosynthetic interface friction angle and adhesion. Hence, interface friction angle and adhesion are the important parameters for PSS next to normal stress.

- It is known that the normal stress and dry density are correlated and thus the dry density parameter should have come second in the ranking, but the connecting weight approach shows the dry density to be the fourth important parameter. In a direct shear box the weight of soil sample becomes insignificant in comparison to the applied normal stress which is acting as a surcharge. For an example Farsakh et al. (2007) used a large size shear box consisting of an upper box and lower box both having dimensions 300 mm long, 300 mm wide and 65.4 mm deep. The normal stress due to dry density acting on soil–geosynthetic interface comes around 1 kPa where as the normal stresses applied to the clay sample were 25, 50 and 75 kPa.

Hence, the ranking of dry density as fourth important parameter is justified.

- The interface shear failure envelopes generally decreases with the increase in molding moisture contents as relevant in the sensitivity analysis with negative sign as shown in Table 11. The increase in water content develops excess pore water pressure resulting in decrease of PSS. Thus ranking water content to be the least important parameter is justified.

Mozumder and Laskar (2015) also reported that ranking given by Connection weight approach is more realistic and acceptable than the Garson's algorithm.

6 Neural Interpretation Diagram (NID)

The neural interpretation diagram (NID) was proposed by Ozesmi and Ozesmi (1999) for visual interpretation of the connection weights among the neurons. The lines joining the input-hidden and hidden-output neurons in the NID represent the magnitude of weights and their directions. The positive and negative weights are represented by black and gray lines respectively, and the thickness of the lines is proportional to their relative magnitude. The input and output relationship is determined in two steps. The positive input hidden and positive hidden-output weights or a negative input-hidden and negative hidden-output weight depict the positive effect of the input variables. The negative effect of the input variables is depicted by positive input-hidden and negative hidden-output or negative input-hidden and positive hidden-output weights. The input having a direct effect on the output is represented by black circles and that having an inverse effect with gray circles. For the present example the weights are presented in Table 10 and NID is presented in Fig. 5. It is seen from Fig. 5 that the inputs γ, σ_n, c_a and δ have a positive contribution to the Y values and %w has negative effects on the Y value which justifies the physical relationship of the soil–geosynthetic interaction mechanism. It is also seen that with an increase in the moisture content there is an appreciable reduction in interface shear resistance as reported by other researchers (Farrag and Griffin 1993; Farrag 1995; Farsakh et al. 2007). Therefore, it is inferred that γ, σ_n, c_a and δ are directly and %w is inversely proportional to Y value. So it can be concluded that NID is an effective method of indicating the physical relationship between inputs with the output.

7 ANN Model Equation for Predicting PSS Value Based on Trained Neural Network

The mathematical equation as per the ANN relating the input and the output variables suggested by Goh et al. (2005) can be written as

$$Y_n = f_{sig}\left\{ b_0 + \sum_{k=1}^{h}\left[w_k \times f_{sig}\left(b_{hk} + \sum_{i=1}^{m} w_{ik} X_i \right)\right]\right\} \quad (3)$$

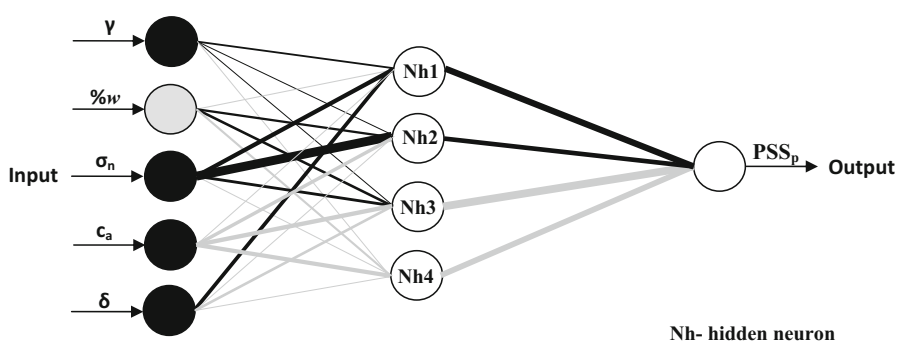

Fig. 5 Neural interpretation diagram of ANN model

where Y_n is the normalized (in the range −1 to 1 in this case) Y value; b_0 is the bias at the output layer; w_k is the connection weight between kth neuron of hidden layer and the single output neuron; b_{hk} is the bias at the kth neuron of hidden layer; h is the number of neurons in the hidden layer; w_{ik} is the connection weight between ith input variable and kth neuron of hidden layer; X_i is the normalized input variable i in the range [−1, 1] and f_{sig} is the sigmoid transfer function.

In this study, an ANN model equation for peak shear stress along soil geosynthetics was established using the values of the weights and biases presented in Table 10 the following expression can be written to finally arrive at a correlation of Y with the input parameters.

$$A_1 = -0.611 + 0.2241\rho - 0.1281w + 0.5307\sigma_n - 0.1079c_a + 0.4599\delta \quad (4)$$

$$A_2 = 0.0486 + 0.0354\rho + 0.2943w + 1.0981\sigma_n - 0.4282c_a - 0.0225\delta \quad (5)$$

$$A_3 = -0.3116 + 0.0175\rho + 0.3211w + 0.3505\sigma_n - 0.5339c_a - 0.3239\delta \quad (6)$$

$$A_4 = -0.2448 - 0.1136\rho - 0.2624w - 0.0649\sigma_n - 0.5137c_a - 0.0691\delta \quad (7)$$

$$B_1 = 0.7687 \times \frac{e^{A_1} - e^{-A_1}}{e^{A_1} + e^{-A_1}} \quad (8)$$

$$B_2 = 0.5707 \times \frac{e^{A_2} - e^{-A_2}}{e^{A_2} + e^{-A_2}} \quad (9)$$

$$B_3 = -0.9582 \times \frac{e^{A_3} - e^{-A_3}}{e^{A_3} + e^{-A_3}} \quad (10)$$

$$B_4 = -0.7049 \times \frac{e^{A_4} - e^{-A_4}}{e^{A_4} + e^{-A_4}} \quad (11)$$

$$C_1 = -0.1726 + B_1 + B_2 + B_3 + B_4 \quad (12)$$

$$Y_n = \frac{e^{C_1} - e^{-C_1}}{e^{C_1} + e^{-C_1}} \quad (13)$$

The Y_n value as obtained from Eq. (13) is in the range [−1, 1] and this needs to be denormalized as

$$Y = 0.5(Y_n + 1)(Y_{max} - Y_{min}) + Y_{min} \quad (14)$$

where Y_{max} and Y_{min} are the maximum and minimum values of Y respectively in the data set.

8 Conclusions

The following are the conclusions from the above studies:

- Out of four learning algorithms Bayesian regularization back propagation learning algorithm is used for its better generalization to the training and testing data and lowest statistical error.
- ANN model with Bayesian regularization back propagation training algorithm outperforms MVR model in predicting the PSS.
- Based on sensitivity analysis both the algorithms, namely Garson's and connection weight approaches rank σ_n as the most important parameter influencing PSS prediction followed by γ, $\%w$, c_a and δ.
- MVR model shows that σ_n, c_a and δ are the significant parameters for PSS prediction.
- According to Connection weight approach, out of five input parameters moisture content (%w) is the least important parameter influencing PSS prediction.
- NID demonstrates the negative or inverse effect of moisture content (%w) on the PSS prediction i.e. with increase in moisture content PSS decreases.
- The superiority of ANN model over MVR model in PSS prediction can be attributed to its flexibility and adaptability in generalizing the data.
- Compared to Garson's algorithm, Connection weight approach is capable of identifying the true importance of input variables in PSS prediction.
- A model equation is presented based on the trained weights of the ANN.

References

Abdel-Baki MS, Raymond GP (1994) Numerical analysis of geotextile reinforced soil slabs. In: Fifth international conference on geotextiles, geomembranes and related products, Singapore

Ajdari M, Habibagahi G, Ghahramani A (2012) Predicting effective stress parameter of unsaturated soils using neural

networks. Comput Geotech 40:89–96. doi:10.1016/j.compgeo.2011.09.004
Andrawes KZ, Mcgown A, Wilson-Fahmy RF, Mashhour MM (1982) The finite element method of analysis applied to soil–geotextile systems. In: Second international conference of geotextiles, Las Vegas, USA, pp 695–700
Basudhar PK, Dixit PM, Gharpure A, Deb K (2008) Finite element analysis of geotextile-reinforced sand-bed subjected to strip loading. Geotext Geomembr 26:91–99. doi:10.1016/j.geotexmem.2007.04.002
Box GEP, Tiao GC (1973) Bayesian inference in statistical analysis. Addison-Wesley, Reading
Burd HJ, Brocklehurst CJ (1990) Finite element studies of the mechanics of reinforced unpaved roads. In: Proceedings of the fourth international conference on geotextiles, geomembranes and related products, The Hauge, Netherlands, pp 217–221
Caudill M (1989) Neural Networks Primer. San Francisco (CA), Miller Freeman Publications
Caudill M, Butler C (1992) Understanding neural networks: computer explorations, vols 1 and 2. The MIT Press, Cambridge
DARPA (1988) Neural network study. M.I.T., Lincoln, Laboratory, Lexington
Das SK, Basudhar PK (2006) Undrained lateral load capacity of piles in clay using artificial neural network. Comput Geotech 33(8):454–459. doi:10.1016/j.compgeo.2006.08.006
Das SK, Basudhar PK (2008) Prediction of residual friction angle of clays using artificial neural network. Eng Geol 100(3–4):142–145. doi:10.1016/j.enggeo.2008.03.001
Das SK, Samui P, Sabat AK (2011) Density and unconfined compressive strength of cement stabilized soil. Geotech Geol Eng 29:329–342. doi:10.1007/s10706-010-9379-4
Farrag K (1995) Effect of moisture content on the interaction properties of geosynthetics. In: Geosynthetics'95, pp 1031–1041
Farrag K, Griffin P (1993) Pull-out testing in cohesive soils, geosynthetic soil reinforcement testing procedures. ASTM STP No. 1190, West Conshohocken, PA, pp 76–89
Farrag K, Morvant M (2003a) Evaluation of interaction properties of geosynthetics in cohesive soils: LTRC reinforced-soil test wall, Rep. No. FHWA/LA 03/379. Louisiana Transportation Research Center, Baton Rouge, LA
Farrag K, Morvant M (2003b) Evaluation of interaction properties of geosynthetics in cohesive soils: lab and field pullout tests, Rep. No. FHWA/LA 03/380. Louisiana Transportation Research Center, Baton Rouge, LA
Farsakh MA, Coronel J, Tao M (2007) Effect of soil moisture content and dry density on cohesive soil–geosynthetic interactions using large direct shear tests. J Mater Civ Eng ASCE 19:540–549. doi:10.1061/(ASCE)0899-1561(2007)19:7(540)
Fletcher R (2000) Practical methods of optimization. Wiley, New York
Garson GD (1991) Interpreting neural-network connection weights. Artif Intell Expert 6(7):47–51
Gens A, Carol I, Alonso EE (1988) An interface element formulation for the analysis of soil–reinforcement interaction. Comput Geotech 7:133–151. doi:10.1016/0266-352X(89)90011-6
Goh ATC (1994) Seismic liquefaction potential assessed by using neural networks. J Geotech E 120(9):1467–1480. doi:10.1061/(ASCE)0733-9410(1994)120:9(1467)
Goh ATC (1995) Empirical design in geotechnics using neural networks. Geotechnique 45(4):709–714
Goh ATC, Kulhawy FH, Chua CG (2005) Bayesian neural network analysis of undrained side resistance of drilled shafts. J Geotech Geoenviron Eng ASCE 131(1):84–93. doi:10.1061/(ASCE)1090-0241(2005)131:1(84)
Gull SF (1988) Bayesian inductive inference and maximum entropy. In: Ericson GJ, Smith CR (eds) Maximum entropy and Bayesian methods in science and engineering, vol 1. Kluwer, Norwell, pp 53–74
Kanayama M, Rohe A, Paassen LA (2014) Using and improving neural network models for ground settlement prediction. Geotech Geol Eng 32:687–697. doi:10.1007/s10706-014-9745-8
Khandelwal M, Singh TN (2010) Prediction of macerals contents of Indian coals from proximate and ultimate analyses using artificial neural networks. Fuel 89:1101–1109. doi:10.1016/j.fuel.2009.11.028
Lee IM, Lee JH (1996) Prediction of pile bearing capacity using artificial neural networks. Comput Geotech 18(3):189–200
Lippman RP (1987) An introduction to computing with neural nets. IEEE ASSP Mag 4:4–22. doi:10.1109/MASSP.1987.1165576
Lopes ML (2002) Soil–geosynthetic interaction. In: Shukla SK (ed) Geosynthetics and their applications. Thomas Telford, London
Love JP, Burd HJ, Milligan GWE, Houlsby GT (1987) Analytical and model studies of reinforcement of a layer of granular fill on a soft clay subgrade. Can Geotech J 24:611–622
MacKay DJC (1991) Bayesian methods for adaptive models. Ph.D. Dissertation, California Institute of Technology, California
Maji VB, Sitharam TG (2008) Prediction of elastic modulus of jointed rock mass using artificial neural networks. Geotech Geol Eng 26:443–452. doi:10.1007/s10706-008-9180-9
Minsky M, Papert S (1969) An introduction to computational geometry. MIT Press, Cambridge. ISBN 0-262-63022-2
Mitchell JK, Seed RB, Seed HB (1990) Kettleman Hills waste landfill slope failure, I: Liner-system properties. J Geotech Eng 116(4):647–668. doi:10.1061/(ASCE)0733-9410(1990)116:4(647)
Moller MF (1993) A scaled conjugate gradient algorithm for fast supervised learning. Neural Netw 6:525–533. doi:10.1016/S0893-6080(05)80056-5
Monjezi M, Singh TN, Khandelwal M, Sinha S, Singh V, Hosseini I (2006) Prediction and analysis of blast parameters using artificial neural network. Noise Vib Control Worldw 37:8–16. doi:10.1260/095745606777630323
Monjezi M, Hasanipanah M, Khandelwal M (2013) Evaluation and prediction of blast-induced ground vibration at Shur River Dam, Iran, by artificial neural network. Neural Comput Appl 22:1637–1643. doi:10.1007/s00521-012-0856-y
Mozumder RA, Laskar AI (2015) Prediction of unconfined compressive strength of geopolymer stabilized clayey soil

using artificial neural network. Comput Geotech 69:291–300. doi:10.1016/j.compgeo.2015.05.021

Neal RM (1992) Bayesian training of back-propagation networks by the hybrid Monte Carlo method. Technical Rep. No. CRG-TG-92-1, Dept. of Computer Science, Univ. of Toronto, Toronto

Olden JD, Jackson DA (2002) Illuminating the ''black box'': a randomization approach for understanding variable contributions in artificial neural networks. Ecol Model 154:135–150. doi:10.1016/S0304-3800(02)00064-9

Ozesmi SL, Ozesmi U (1999) An artificial neural network approach to spatial modeling with inter specific interactions. Ecol Model 116:15–31. doi:10.1016/S0304-3800(98)00149-5

Park HI, Lee SR (2011) Evaluation of the compression index of soils using an artificial neural network. Comput Geotech 38:472–481. doi:10.1016/j.compgeo.2011.02.011

Poran CJ, Herrmann LR, Romstad KM (1989) Finite element analysis of footings on geogrid-reinforced soil. In: Proceedings of geosynthetics, San Diego, USA, pp 231–242

Poulos HJ, Davis EH (1974) Elastic solution for the soil and rock mechanisms. Wiley, New York

Rumelhart DE, Hinton GE, Williams RJ (1986) Learning internal representation by error propagation. In: Rumelhart DE, McCleland JL (eds) Parallel distribution processing: explorations in the microstructure of cognition, vol 1. MIT Press, Cambridge, pp 318–362

Sakellariou MG, Ferentinou MD (2005) A study of slope stability prediction using neural networks. Geotech Geol Eng 23:419–445. doi:10.1007/s10706-004-8680-5

Sarkar K, Tiwary A, Singh TN (2010) Estimation of strength parameters of rock using artificial neural networks. Bull Eng Geol Environ 69:599–606. doi:10.1007/s10064-010-0301-3

Shahin MA, Maier HR, Jaksa MB (2004) Data division for developing neural networks applied to geotechnical engineering. J Comput Civ Eng 18(2):105–114. doi:10.1061/(ASCE)0887-3801(2004)18:2(105)

Singh TN, Kanchan R, Verma AK, Saigal K (2005) A comparative study of ANN and neuro-fuzzy for the prediction of dynamic constant of rockmass. J Earth Syst Sci 114:75–86

Sinha SK, Wang MC (2008) Artificial neural network prediction models for soil compaction and permeability. Geotech Geol Eng 26:47–64. doi:10.1007/s10706-007-9146-3

Sivapullaiah PV, Guru Prasad B, Allam MM (2009) Modeling sulfuric acid induced swell in carbonate clays using artificial neural networks. Geomech Eng 1(4):307–321. doi:10.12989/gae.2009.1.4.307

Sobhani J, Najimi M, Pourkhorshidi AR, Parhizkar T (2010) Prediction of the compressive strength of no-slump concrete: a comparative study of regression, neural network and ANFIS models. Constr Build Mater 24:709–718. doi:10.1016/j.conbuildmat.2009.10.037

Sonmez H, Gokceoglu C, Nefeslioglu HA, Kayabasi A (2006) Estimation of rock modulus: for intact rocks with an artificial neural network and for rock masses with a new empirical equation. Int J Rock Mech Min 43:224–235. doi:10.1016/j.ijrmms.2005.06.007

Verschuuren G (2007) Excel 2007 for scientists and engineers. Holy Macro! Books, Uniontown

Wilson-Fahmy RF, Koerner RM (1993) Finite element modeling of soil geogrid interface with application to the behavior of geogrids in a pullout loading conditions. Geotext Geomembr 12:479–501. doi:10.1016/0266-1144(93)90023-H

Yamamoto K, Otani J (2002) Bearing capacity and failure mechanism of reinforced foundations based on rigid-plastic finite element formulation. Geotext Geomembr 20:367–393. doi:10.1016/S0266-1144(02)00031-6

Yaprak H, Karaci A, Demir I (2013) Prediction of the effect of varying cure conditions and w/c ratio on the compressive strength of concrete using artificial neural networks. Neural Comp Appl 22:133–141. doi:10.1007/s00521-011-0671-x